Musculoskeletal modelling in dogs: challenges and future perspectives

Billy Dries[1]; Ilse Jonkers[2]; Walter Dingemanse[1]; Benedicte Vanwanseele[2]; Jos Vander Sloten[3]; Henri van Bree[1]; Ingrid Gielen[1]

[1]Department of Medical Imaging of Domestic Animals and Orthopedics of Small Animals, Faculty of Veterinary Medicine, Ghent University, Merelbeke, Belgium; [2]Human Movement Biomechanics Research Group, Faculty of Kinesiology and Rehabilitation Sciences, KU Leuven, Leuven, Belgium; [3]Biomechanics Section, Faculty of Engineering Science, KU Leuven, Leuven, Belgium

Keywords
Musculoskeletal, modelling, dogs, parameters, techniques

Summary
Musculoskeletal models have proven to be a valuable tool in human orthopaedics research. Recently, veterinary research started taking an interest in the computer modelling approach to understand the forces acting upon the canine musculoskeletal system. While many of the methods employed in human musculoskeletal models can applied to canine musculoskeletal models, not all techniques are applicable. This review summarizes the important parameters necessary for modelling, as well as the techniques employed in human musculoskeletal models and the limitations in transferring techniques to canine modelling research. The major challenges in future canine modelling research are likely to centre around devising alternative techniques for obtaining maximal voluntary contractions, as well as finding scaling factors to adapt a generalized canine musculoskeletal model to represent specific breeds and subjects.

Correspondence to:
Billy Dries
Department of Medical Imaging of Domestic Animals and Orthopedics of Small Animals
Faculty of Veterinary Medicine
Ghent University
Salisburylaan 133
Merelbeke 9820
Belgium
Phone: +32 926 47761
E-mail: billy.dries@ugent.be

Vet Comp Orthop Traumatol 2016; 29: 181–187
http://dx.doi.org/10.3415/VCOT-15-08-0133
Received: August 5, 2015
Accepted: February 24, 2016
Epub ahead of print: April 22, 2016

Introduction

Orthopaedic conditions are often related to the forces that act upon the musculoskeletal system. A non-physiological distribution of forces within the musculoskeletal system can be one of the contributing factors to disorders such as osteochondrosis, ligament rupture, and hip dysplasia, all three of which are known to have multifactorial aetiologies (1–3).

A better understanding of the forces acting upon the musculoskeletal system would allow further insights into the onset and progression of these orthopaedic conditions. However, to date, it has been impossible to non-invasively measure the internal loadings of living dogs during locomotion. In human applications, this problem is solved by combining three-dimensional motion capture, a musculoskeletal model and dynamic simulations of motion. The use of this methodology has already yielded several applications and is a widely accepted tool in the field of human movement biomechanics.

Musculoskeletal models represent the musculoskeletal structure as a chain of rigid body segments connected through physiological joints and actuated by musculo-tendon actuators. These musculoskeletal models are typically combined with data on three-dimensional segmental motion and ground reaction force data (measured using motion capture techniques and force plates respectively) to perform inverse dynamics simulations. These inverse dynamics simulations calculate the forces and moments acting at the joints based on experimentally measured external forces, including gravity and inertia, and segmental acceleration (4). In combination with an optimization formulation, muscle excitations can be calculated that can then be validated by electromyography measurements (5, 6). These muscle excitations then allow the calculation of individual muscle forces as well as the resulting joint reaction forces. An optimization formulation considers the model as a redundant dynamic system, for which the muscle force sharing problem is solved by an optimization algorithm (5). Therefore, the summed individual muscle moments need to reproduce the desired joint moments while optimizing a performance criterion, which is in most cases a minimization of the muscle activation. This is important as there are more muscles available than necessary to drive a given motion, and muscles will rarely be stimulated to maximal activation.

Alternatively to inverse dynamics models, electromyography-driven forward dynamics simulations take the *in vivo* measured muscle activation of muscles and applies them as input to the simulation to calculate muscle forces (7). The downsides of this approach relate to the difficulty to non-invasively measure electromyography

on all muscles defined in a segment, as well as an incomplete understanding of the transformation of the muscle activation into muscle force (8).

Musculoskeletal models have been extensively used to explore clinical questions in human orthopaedic medicine. Musculoskeletal models have substantially advanced the understanding of normal and pathological movement, and are currently being used to define assistive devices that restore function following an injury and for preoperative planning, such as for simulation of tendon transfers, tendon lengthening, and osteotomies (9-13).

As part of a multi-scale modelling workflow, muscle and joint contact forces calculated by musculoskeletal models have been used in finite element modelling. This includes analysing the forces acting in joints and including cartilage, designing implants and prosthesis, studying patterns of growth and development, studying the elastic properties of bone, and examining the mechanisms behind bone failure or fracture (14-18).

The use of musculoskeletal modelling to better understand the loading patterns of the musculoskeletal system, and its relationship to specific orthopaedic conditions in veterinary medicine in general and canine orthopaedics in specific, is currently being explored. Musculoskeletal models were already developed for the cat, rat, rabbit and horse (19-22). The modelling approach makes a number of assumptions which limit its applicability. These assumptions will be elaborated upon in the following sections.

This review article gives an overview of the caveats that currently limit the use of musculoskeletal models in canine research and indicates the appropriate experimental methods required to collect the required parameters. Muscle and tendon modelling will receive more attention in this review because canine muscle and tendon parameters are expected to differ strongly from those of human muscles, and because not all techniques employed in human muscle modelling are applicable to canine muscle modelling.

Methodological review: modelling bone and joint

Musculoskeletal models represent the bones as rigid bodies (segments) interconnected by frictionless joints. Body segments are defined as rigid geometrical representations of the bone with a local coordinate system. Due to the complex nature of specific body segments (e.g. the canine foot), or in case model simplicity is mandatory for computational reasons, non-rigid body parts consisting of multiple segments are sometimes modelled as one rigid segment. An orthogonal coordinate system is constructed for each body segment, in which an origin and three-dimensional axis are defined based on anatomical bone landmarks (23). In human musculoskeletal models, the International Society of Biomechanics convention is used to generalize the coordinate system definitions (24).

The centre of mass represents the point around which the mass of the segment is balanced, and is used to simplify mechanics calculations. The segment's moment of inertia determines its resistance to change in angular velocity, and is an important parameter in determining how segments react to the forces and consequent moments applied on them. Typically, a fixed three-dimensional centre of mass location and constant three-dimensional inertial properties are defined for each segment, therefore omitting their changes due to segmental deformation caused by muscle contraction during locomotion.

While some joints can perform complex three-dimensional sliding and rotating motions, in musculoskeletal models, they are usually represented as simple hinges (e.g. knee, ankle, elbow) or as ball-and-socket joints (e.g. hip and shoulder) and are always assumed to be frictionless (25). Simplified representations of the joints are common given the difficulty to accurately measure three-dimensional joint kinematics using skin marker-based motion capture that is often used as input for the musculoskeletal model. The simplified joint definitions and constant dynamic parameters of the segments (e.g. inertia, centre of mass) are some of the inherent limitations of the modelling workflow.

Experimental methods to obtain skeletal parameters

Three-dimensional bone geometry can be acquired through x-ray computed tomography (CT) scanning or magnetic resonance imaging (MRI). These techniques have been shown to have equivalent accuracy (26). The images acquired can be either manually segmented or processed through reconstruction algorithms to create a three-dimensional geometrical model (27). Determination of segmental mass distribution and inertial parameters can be acquired *in vitro* through dedicated experimental techniques, as well as based on medical imaging (e.g. MRI or CT) (28-30).

Although coordinate systems have already been formulated for the canine forelimb, hindlimb and neck, to date no conventions on coordinate systems have been established (31–33). Inertial parameters can be based on the density data and distribution of masses acquired through CT scans and MRI.

The arthrokinematics (i.e. the kinematics of the joints) can be determined either by defining the kinematic relationships of the segments by the use of external marker systems or, alternatively, by analysing the geometry of the joint surfaces (34). This joint surface geometry can be acquired through a combination of MRI, CT, and micro-CT scanning (35).

Methodological review: modelling muscle and tendon

In musculoskeletal models, a muscle is modelled as a line of action between two attachment sites on the bone surfaces. This represents the line of action of the muscle force acting onto the segments (▶Figure 1). An attachment site is modelled as a single coordinate point on the segment. For muscles with large attachment sites, one or multiple centroids can be defined, representing the lines of action of functional subdivisions.

Parametrizing muscle geometry involves defining three-dimensional coordinates of the origin and insertion of the

musculo-tendon actuator on the bone surface, as well as accounting for the curvature around the bones that interferes with a straight line muscle assumption. Accounting for the curvature of musculo-tendon actuators requires definition of the shape and position of wrapping surfaces. This information can be collected through dissection, imaging techniques, or both, and requires thorough knowledge of canine muscle anatomy. A limitation of the modelling approach is that it only accounts for functionally important curvature of the musculo-tendon actuator paths using "via points" representing muscle wrapping along the bone surface or muscular structures.

Force production of the musculo-tendon actuators is typically modelled using a hill-type model (▶Figure 2) (36). The force generated by the contractile element (F^{CE}) represents the active force generated by the crossbridges and is dependent on three properties: the level of muscle activation, the active force-length relationship, and the force-velocity relationship. The force generated by the passive element (F^{PE}) represents the elastic stretching force generated by the muscle when stretched beyond its optimal fibre length. Similar to the muscle's passive element, the tendon is modelled to behave elastically. The force output of the series elastic element F^{T} increases with lengthening of the tendon. The effective force output of the musculo-tendon actuator (F^{MT}) constitutes the summation of the force output of the tendon and the total force output of the muscle corrected for the pennation angle (α), representing the angle at which the muscle fibres are implanted into the tendon. The optimal fibre pennation angle (α_o) impacts the amount of active force production that is transferred along the line of the tendon. This effect is important for angles exceeding 20° (37).

Using the Hill-model, only four parameters are required to model the force production of a specific musculo-tendon actuator. These include the optimal muscle fibre length (L^{M}_{o}; i.e. the muscle fibre length at optimal sarcomere length), the maximal isometric muscle force (F^{M}_{o}; i.e. the maximal force generated by the muscle at L^{M}_{o}), the optimal fibre pennation angle (α_o; i.e. the pennation angle at L^{M}_{o}) and the tendon slack length (L^{T}_{s}).

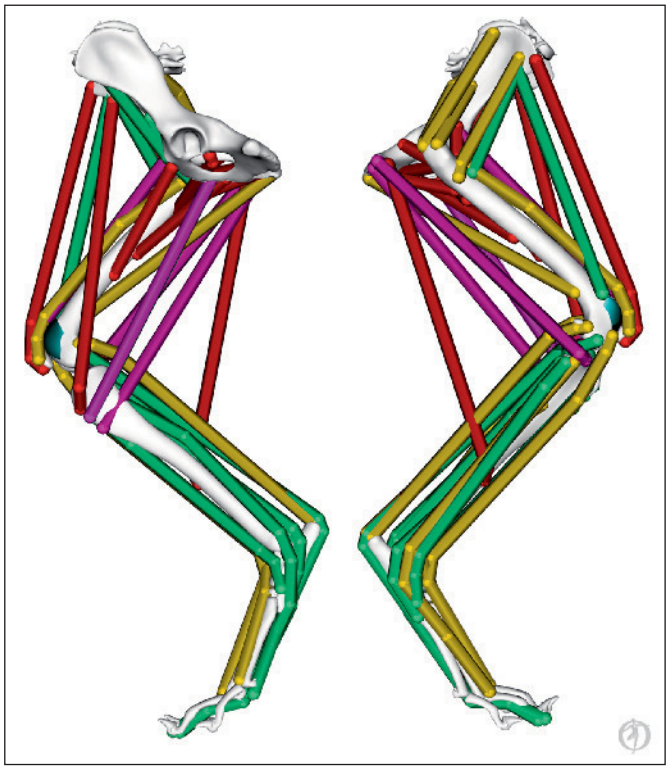

Figure 1 Image of a canine hindlimb musculoskeletal model consisting of three segments: pelvis, femur, tibia/fibula and a tarso-metatarsal-phalangeal segment. The musculo-tendon actuators are represented by actuator lines connecting origin and insertion points. Extensor muscles are displayed in yellow, flexor muscles in blue, muscles with both these functions in purple, and muscles with other functions in red. **Left:** medial aspect of the model; **Right:** lateral aspect.

Computer modelling employs a generic muscle-tendon based model that constitutes dimensionless (normalized) formulations of the muscle properties. This generic model can be adjusted to represent a specific musculo-tendon actuator by using the measurable parameters described in the following sections. The following for-

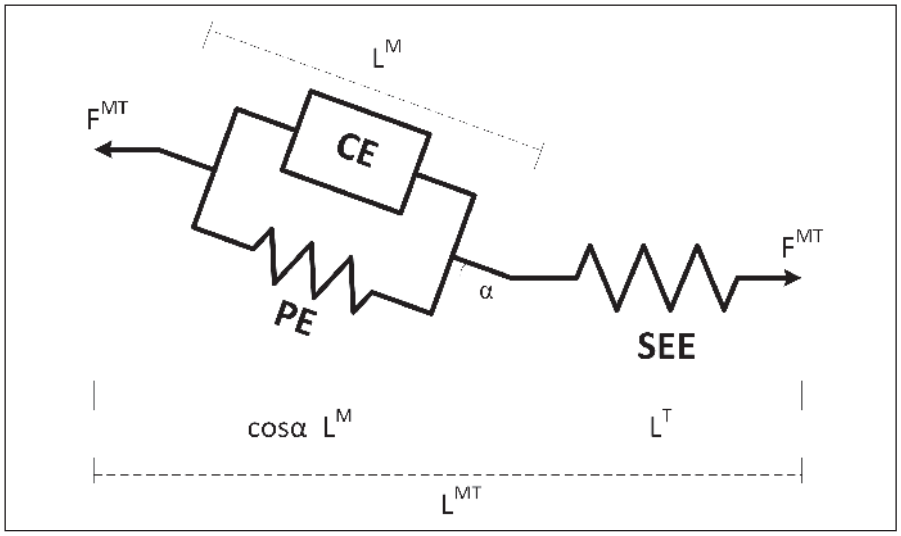

Figure 2 Hill-type model of the musculo-tendon actuator muscle with a contractile element (CE), a passive element (PE) and a series elastic element (SEE). The CE has input from activation dynamics (a(t)), fibre length (L^{M}) and shortening velocity (v^{m}). The PE has input from L^{M}, and the SEE has input from L^{T}. The total musculo-tendon length is the sum of L^{T} and L^{M} times the cosine of the pennation angle α. Only activation is an external input variable, and the force F^{MT} is the only output variable transmitted to each end of the actuator.

mula describes how the previously mentioned parameters can be used to calculate forces in a musculo-tendon-model (38):

$$F^M_o\,(a\,f^L[\sim L^M]\;\; f^V[\sim v^M] + f^{PE}[\sim L^M]\,)\,\cos\alpha - F^M_o f^T(\sim L^T) = 0$$

Where 'a' represents the level of muscle activation, the only external input for a muscle model. The contractile element (CE) is represented by both $f^L[\sim L^M]$, which yields a muscle force based on its fibre length (normalized by L^M_o), and $f^V[\sim v^M]$, which yields a muscle force based on shortening velocity (normalized by a constant maximal shortening velocity). The passive element (PE) is represented by $f^{PE}(\sim L^M)$, which represents the passive force yielded at $L^M > L^M_o$. The portion $f^T(\sim L^T)$ yields a tendon force based on its tendon length (normalized by L^T_s).

Experimental methods to obtain musculo-tendon parameters for muscle force production

In order to customize existing generic muscle models to represent canine musculo-tendon actuators, experimental values for the above mentioned parameters need to be acquired in dogs. This section will review the methods for acquiring these methods in dogs as well as the parameters that are already available in literature.

Optimal fibre length

In order to calculate optimal fibre length, a species-specific measurement of optimal sarcomere length (i.e. the length at which myofilaments show an optimal overlap) has to be obtained (39). Most models use a species-specific value for optimal sarcomere length, which can be determined by measuring the myofilament length (40). While myosin filament length shows little variation between vertebrates, the actin filament length can vary considerably between species (40). In case the actin filament length was unknown, some studies have used the optimal sarcomere length of a closely related species (41). However, to our knowledge no studies have investigated the validity of this approach. While values of optimal sarcomere length have already been determined for cats, no values on optimal sarcomere length have been published for canine muscles (42).

Alternatively, optimal sarcomere length can be calculated as twice the actin (thin) filament length added to half the width of the bare zone (41). These can be measured using transmission electron microscopy (TEM) (42). To compensate for filament shrinkage during the fixation process, a shrinkage factor can be calculated based on a constant length assumption of the myosin filament length across mammals, i.e. 1.6 µm (42).

With an experimentally determined species-specific optimal sarcomere length, a muscle-specific value for optimal fibre length can be calculated from the measured fibre length and its sarcomere length at that fibre length.

These measures for fibre length and sarcomere length can be obtained by fixating dissected muscles and treating them to loosen the muscle fibres (43). Thereafter, individual muscle fibres can be extracted and their length measured. The sarcomere lengths can subsequently be measured through either light microscopy, which has a limited resolution, laser diffraction, which immediately measures the average sarcomere length, or TEM, which has a significantly higher resolution and accuracy than other techniques, but is more expensive and labour-intensive (31, 44, 45).

In vivo measurements of fibre length can be obtained through ultrasound, and can be combined with measurements of sarcomere length achieved through intraoperative laser diffraction on a muscle fibre exposed through surgery (46, 47). However, these *in vivo* techniques for obtaining optimal fibre length can only be applied to easily accessible muscles directly under the surface of the skin.

Optimal fibre lengths have already been reported for the canine neck musculature (31). However, these values have been calculated based on values for optimal sarcomere length of cat muscles. Fibre length has also been reported for the canine forelimb and hindlimb musculature (33, 43). However, these measurements were not accompanied by sarcomere lengths, and therefore do not allow us to calculate optimal fibre length.

Optimal fibre pennation angle

Optimal pennation angle is the pennation angle at optimal fibre length. However, many studies use pennation angle data that is not necessarily measured at optimal fibre length. The standard methods for measuring pennation angle are dissection or ultrasound (46). Ultrasound has the advantage that pennation angles can be measured for specific fibre lengths.

Pennation angles for the canine forelimb and neck musculature have been reported in detail, ranging from 0° to 40° (31, 33). While, no values for pennation angles for the canine hindlimb musculature pennation angles have been reported, it was noted that the measured pennation angles of the (upper) canine hindlimb muscles are below 20° (43). Musculoskeletal models often assume pennation angles below 20° to be equal to 0° as they do not significantly alter the modelled musculo-tendon actuator's force output (37).

Most musculoskeletal models consider the pennation angle as constant, while this parameter in reality changes during muscle shortening and lengthening. As it is methodologically challenging to experimentally determine the changes in muscle pennation angle during contraction, the use of a constant pennation angle is another limitation of current musculoskeletal models.

Maximal isometric muscle force

Muscle size measurements are often used to determine the maximal muscle force output. As these measurements can be obtained using different methods, limited standardization has introduced significant variability between studies. The muscle cross-sectional area relates to the number of sarcomeres placed in parallel and is a measure for the maximal force that can be achieved by a muscle during full activation. Physical cross sectional area (PCSA) represents the surface area of the plane parallel to the direction of the muscle fibres. The maximal isometric muscle force F^M_o can be calculated from the PCSA and the optimal fibre length L^M_o via the following formula:

$$P_o = P_{sp} \times PCSA = P_{sp} \times \cos\alpha\,(V^M/L^M_o) = P_{sp} \times \cos\alpha\,(m^M \times \rho^M / L^M_o)$$

Where V^M represents the muscle volume, the constants P_o and P_{sp} respectively represent the maximal and the specific muscle tension, m^M the muscle mass, and ρ^M the muscle density (1.056 g/cm^3 for mammalian muscle tissue). The maximal muscle tension P_o can then be used as a value for maximal isometric muscle force F^M_o. Based on this formula, the muscle's maximal force can be determined by its mass (determined through dissection) or volume (determined through CT or MRI) if a reliable value for specific muscle tension is available.

The PCSA of muscles have been reported for the canine neck, forelimb and hindlimb musculature (31, 33, 43). However, these cannot yet be used to reliably calculate maximal muscle force production as no values for canine specific muscle tension have been published to date. In general, values for specific muscle tension in isolated animal muscles are assumed to be around ~225 kN/m^2 (48). However, values of specific muscle tension reported in the literature vary largely, ranging between 59 kN/m^2 and 682 kN/m^2, both within and between species (49, 50). Obtaining a value for specific muscle tension in dogs can be achieved by directly measuring maximal isometric muscle force in canine muscles in combination with measures of muscle volume acquired through MRI and muscle fibre length through ultrasound.

In humans, maximal isometric muscle force, also referred to as peak isometric muscle force, is most commonly measured through isometric or isotonic maximum voluntary contraction (51). This has proven to be a reliable method to obtain *in vivo* measurements of maximal isometric voluntary muscle force generation. In dogs, this method cannot readily be used as it requires the subject to induce voluntarily a maximal, selective contraction. Alternatively, a maximal muscle contraction can be induced using functional electric stimulation either by stimulating the connecting nerve trunk (rarely an option) or by stimulating the muscle directly (49).

Tendon slack length

Assuming a generic length-tension relationship for tendon stiffness, the tendon slack length is the only parameter necessary to model the tendon force generation. For some tendons, the slack length is obtained through ultrasound by identifying the joint angle at which passive musculotendon force generation starts. This yields an *in vivo* value for tendon slack length of a specific musculo-tendon actuator (52). However this is a time-consuming process which can only be used in musculo-tendon actuators that can easily be visualized and have long enough tendons. Because tendon slack length is a difficult parameter to obtain, models often make assumptions on tendon slack length based on the musculotendon actuator's excursion length or on the musculo-tendon actuator's maximal elongation L^{MT}_o and its optimal fibre length L^M_o (53, 54).

The tendon slack length L^T_s may prove to be the most challenging parameter to measure in dogs. The use of model-based assumptions for L^T_s may be the most straightforward method of obtaining values for L^T_s, providing they are validated for a number of representative canine tendons.

The assumption of a generic length-tension relationship of the tendon is a significant limitation of the modelling approach, as their elastic properties differ significantly (55). This highlights the need for experimental determination of individual tendon elastic properties.

Discussion

The goal of this review was to summarize the important concepts of musculoskeletal model, and introduce the technique to those less familiar with it in the field. Compared with state of the art research in the field of human movement biomechanics, the current review highlights the potential and the steps required to further the use of musculoskeletal modelling in canine orthopaedics. From a review of the literature, it becomes clear that although dedicated methodology exists, only a limited number of parameters have been identified for dogs. Whereas it is to be expected that techniques to derive the bone-related parameters can be easily transferred, the experimental quantification of muscle and tendon parameters will require further dedicated research, in particular on the following topics.

Firstly, dedicated values for myofilament length are needed to calculate an optimal fibre length for canine muscle actuators. Secondly, the determination of the maximal isometric muscle forces will be restricted to a muscle size based methodology. As voluntary isolated contractions cannot be elicited in dogs, validation of these muscle size-based estimates may be difficult.

The following two aspects need to be carefully considered when elaborating a canine-specific musculoskeletal model workflow. Firstly, in contrast to humans, the relative importance of the muscle versus tendon parameters in the musculo-tendon force production may be largely different in dogs. As in other digitigrade animals, most canine limb muscles are located proximally with long tendons connecting to the distal parts of the skeleton. This spatial distribution of muscles will limit the inertial moment of the limb. Furthermore, the tendons will have an important function in transferring the active muscle force production as a recoil mechanism that stores and releases energy during locomotion. Therefore, the parameterization of the tendon properties may prove to be more important in a canine musculoskeletal model compared to human musculoskeletal models.

Secondly, whereas in humans scaling of a generic model and its parameters was widely accepted, current research stresses the importance of a subject specific modelling approach (56). The importance of a subject- or breed-specific musculoskeletal model as opposed to a generalized musculoskeletal model may prove even more important in canine musculoskeletal models. A major challenge will be the development of generic model based on a "standard" body type, and a set of scaling factors that allow adaptation of this model to represent different breeds. This may prove difficult as breed-specific differences in muscle and tendon parameters and the anatomical differences between these breeds cannot simply be linked to currently employed body size indices such as weight or the commonly used "body condition score" (57). It may also be likely that different scaling factors need to be developed for dif-

ferent parameters. The PCSA and inertial parameters for instance may scale better with measures of body weight, while muscle fibre length and tendon slack length may scale better with a value for limb length as a scaling factor.

To conclude, since dogs are used for many specific purposes (aiding the disabled, assisting police and the military, and herding) that require a large investment of both time and money that go into the training of individual dogs, early detection and better understanding of the risk for afflictions such as osteochondrosis and hip dysplasia may prevent large investments into potentially unhealthy individuals. Building on the research insights gained from human musculoskeletal model applications, the creation of elaborate research techniques seems justified as diagnostic techniques allowing better screening methods of detecting individuals at greater risk of orthopaedic afflictions later on in life. However, musculoskeletal models in dogs may not prove to be as simple as copying the techniques and conventions employed in humans. Specific techniques for determining the muscle-tendon parameters and especially of the maximal isometric force may have to be developed because canine research subjects cannot be asked to perform voluntary contractions of specific muscle groups.

Conflict of interest statement

None of the authors of this paper has a financial or personal relationship with other people or organizations that could inappropriately influence or bias the content of the paper.

References

1. Kuroki K, Cook JL, Stoker AM, et al. Characterizing osteochondrosis in the dog: Potential roles for matrix metalloproteinases and mechanical load in pathogenesis and disease progression. Osteoarthritis Cartilage 2005; 13: 225–234.
2. Whitehair JG, Vasseur PB, Willits NH. Epidemiology of cranial cruciate ligament rupture in dogs. J Am Vet Med Assoc 1993; 203: 1016–1019.
3. Ginja MM, Silvestre AM, Gonzalo-Orden JM, et al. Diagnosis, genetic control and preventive management of canine hip dysplasia: A review. Vet J 2010; 184: 269–276.
4. Koopman B, Grootenboer HJ, de Jongh HJ. An inverse dynamics model for the analysis, reconstruction and prediction of bipedal walking. J Biomech 1995; 28: 1369–1376.
5. Xiang Y, Arora JS, Abdel-Malek K. Optimization-based prediction of asymmetric human gait. J Biomech 2011; 44: 683–693.
6. Snijders CJ, Ribbers MT, de Bakker HV, et al. EMG recordings of abdominal and back muscles in various standing postures: Validation of a biomechanical model on sacroiliac joint stability. J Electromyogr Kinesiol 1998; 8: 205–214.
7. Lloyd DG, Besier TF. An EMG-driven musculoskeletal model to estimate muscle forces and knee joint moments in vivo. J Biomech 2003; 36: 765–776.
8. Buchanan TS, Lloyd DG, Manal K, et al. Estimation of muscle forces and joint moments using a forward-inverse dynamics model. Med Sci Sport Exerc 2005; 37: 1911–1916.
9. Stewart C, Shortland AP. The biomechanics of pathological gait – from muscle to movement. Acta Bioeng Biomech 2010; 12: 3–12.
10. Holzbaur KRS, Murray WM, Delp SL. A model of the upper extremity for simulating musculoskeletal surgery and analyzing neuromuscular control. Ann Biomed Eng 2005; 33: 829–840.
11. Bolsterlee B, Veeger DH, Chadwick EK. Clinical applications of musculoskeletal modelling for the shoulder and upper limb. Med Biol Eng Comput 2013; 51: 953–963.
12. Delp SL, Statler K, Carroll NC. Preserving plantar flexion strength after surgical treatment for contracture of the triceps surae: A computer simulation study. J Orthop Res 1995; 13: 96–104.
13. Arnold AS, Blemker SS, Delp SL. Evaluation of a deformable musculoskeletal model for estimating muscle-tendon lengths during crouch gait. Ann Biomed Eng 2001; 29: 263–274.
14. Carter DR, Wong M. Modelling cartilage mechanobiology. Philos Trans R Soc Lond B Biol Sci 2003; 358: 1461–1471.
15. Himmlová L, Dostálová T, Kácovský A, et al. Influence of implant length and diameter on stress distribution: a finite element analysis. J Prosthet Dent 2004; 91: 20–25.
16. Stevens S, Beaupré GS, Carter DR. Computer model of endochondral growth and ossification in long bones: biological and mechanobiological influences. J Orthop Res 1999; 17: 646–653.
17. van Rietbergen B, Weinans H, Huiskes R, et al. A new method to determine trabecular bone elastic properties and loading using micromechanical finite-element models. J Biomech 1995; 28: 69–81.
18. Pistoia W, van Rietbergen B, Lochmüller E, et al. Estimation of distal radius failure load with micro-finite element analysis models based on three-dimensional peripheral quantitative computed tomography images. Bone 2002; 30: 842–848.
19. Burkholder TJ, Nichols TR. Three-dimensional model of the feline hindlimb. J Morphol 2004; 261: 118–129.
20. Johnson WL, Jindrich DL, Roy RR, et al. A three-dimensional model of the rat hindlimb: musculoskeletal geometry and muscle moment arms. J Biomech 2008; 41: 610–619.
21. Grover DM, Chen AA, Hazelwood SJ. Biomechanics of the rabbit knee and ankle: muscle, ligament, and joint contact force predictions. J Biomech 2007; 40: 2816–2821.
22. Rome L, Sosnicki A, Goble D. Maximum velocity of shortening of three fibre types from horse soleus muscle: implications for scaling with body size. J Physiol 1990; 431: 173–185.
23. Hoy M, Zajac F, Gordon M. A musculoskeletal model of the human lower extremity: the effect of muscle, tendon, and moment arm on the moment-angle relationship of musculotendon actuators at the hip, knee, and ankle. J Biomech 1990; 23: 157–169.
24. Wu G, Siegler S, Allard P, et al. ISB recommendation on definitions of joint coordinate system of various joints for the reporting of human joint motion—part I: ankle, hip, and spine. J Biomech 2002; 35: 543–548.
25. Zajac FE, Winters JM. Modeling musculoskeletal movement systems: joint and body segmental dynamics, musculoskeletal actuation, and neuromuscular control. In: Winters JM, Woo SL-Y, editors. Multiple Muscle Systems. New York: Springer; 1990. pg. 121–148.
26. Van den Broeck J, Vereecke E, Wirix-Speetjens R, et al. Segmentation accuracy of long bones. Med Eng Phys 2014; 36: 949–953.
27. Scheys L, Jonkers I, Schutyser F, et al. Image based methods to generate subject-specific musculoskeletal models for gait analysis. International Congress Series 2005; 1281: 62–67.
28. Clauser CE, McConville JT, Young JW. Weight, Volume, and Center of Mass of Segments of the Human Body. AMRL Technical Report, Wright Patterson Air force Base, Ohio (AMRL-TR-69–70); Natl Tech Inf Serv 1969; 1–112. Available at: http://www.dtic.mil/dtic/tr/fulltext/u2/710622.pdf
29. Yeadon MR, Morlock M. The appropriate use of regression equations for the estimation of segmental inertia parameters. J Biomech 1989; 22: 683–689.
30. Martin PE, Mungiole M, Marzke MW, et al. The use of magnetic resonance imaging for measuring segment inertial properties. J Biomech 1989; 22: 367–376.
31. Sharir A, Milgram J, Shahar R. Structural and functional anatomy of the neck musculature of the dog (Canis familiaris). J Anat 2006; 208: 331–351.
32. Shahar R, Banks-Sills L. Biomechanical analysis of the canine hind limb: calculation of forces during three-legged stance. Vet J 2002; 163: 240–250.
33. Shahar R, Milgram J. Morphometric and anatomic study of the forelimb of the dog. J Morphol 2005; 263: 107–117.
34. Kadaba MP, Ramakrishnan HK, Wootten ME. Measurement of lower extremity kinematics during level walking. J Orthop Res 1990; 8: 383–392.
35. DeFrate LE, Sun H, Gill TJ, et al. In vivo tibiofemoral contact analysis using 3D MRI-based knee models. J Biomech 2004; 37: 1499–1504.
36. Hill AV. The heat of shortening and the dynamic constants of muscle. Proc R Soc London B 1938; 126: 612–745.
37. Zajac FE. Muscle and tendon: properties, models, scaling, and application to biomechanics and motor control. Crit Rev Biomed Eng 1989; 17: 359–411.
38. Millard M, Uchida T, Seth A, et al. Flexing computational muscle: modeling and simulation of musculotendon dynamics. J Biomech Eng 2013; 135: 021005.

39. Barr R, Pandy M. Biomechanics of the Musculoskeletal System. In: Kutz M, editor. Standard Handbook of Biomedical Engineering and Design. New York: McGraw-Hill; 2003. pg. 6.1–6.34.
40. van Leeuwen JL. Optimum power output and structural design of sarcomeres. J Theor Biol 1991; 149: 229–256.
41. Burkholder TJ, Lieber RL. Sarcomere length operating range of vertebrate muscles during movement. J Exp Biol 2001; 204: 1529–1536.
42. Herzog W, Kamal S, Clarke HD. Myofilament lengths of cat skeletal muscle: theoretical considerations and functional implications. J Biomech 1992; 25: 945–948.
43. Shahar R, Milgram J. Morphometric and anatomic study of the hind limb of a dog. Am J Vet Res 2001; 62: 928–933.
44. Lieber RL, Yeh Y, Baskin RJ. Sarcomere length determination using laser diffraction. Effect of beam and fiber diameter. Biophys J 1984; 45: 1007–1016.
45. Goulding D, Bullard B, Gautel M. A survey of in situ sarcomere extension in mouse skeletal muscle. J Muscle Res Cell Motil 1997; 18: 465–472.
46. Chleboun GS, France AR, Crill MT, et al. In vivo measurement of fascicle length and pennation angle of the human biceps femoris muscle. Cells Tissues Organs 2001; 169: 401–409.
47. Lieber RL, Loren GJ, Fridén J. In vivo measurement of human wrist extensor muscle sarcomere length changes. J Neurophysiol 1994; 71: 874–881.
48. Maganaris CN, Baltzopoulos V. Ball D, et al. In vivo specific tension of human skeletal muscle. J Appl Physiol (1985) 2001; 90: 865–872.
49. Powell PL, Roy RR, Kanim P, et al. Predictability of skeletal muscle tension from architectural determinations in guinea pig hindlimbs. J Appl Physiol Respir Environ Exerc Physiol 1984; 1715–1721.
50. Weijs WA, Hillen B. Cross-sectional areas and estimated intrinsic strength of the human jaw muscles. Acta Morphol Neerl Scand 1985; 23: 267–274.
51. Bamman MM, Newcomer BR, Larson-Meyer DE, et al. Evaluation of the strength-size relationship in vivo using various muscle size indices. Med Sci Sports Exerc 2000; 32: 1307–1313.
52. Arampatzis A, Stafilidis S, DeMonte G, et al. Strain and elongation of the human gastrocnemius tendon and aponeurosis during maximal plantarflexion effort. J Biomech 2005; 38: 833–841.
53. Garner BA, Pandy MG. Estimation of musculotendon properties in the human upper limb. Ann Biomed Eng 2003; 31: 207–220.
54. Colacino FM, Rustighi E, Mace BR. Subject-specific musculoskeletal parameters of wrist flexors and extensors estimated by an EMG-driven musculoskeletal model. Med Eng Phys 2012; 34: 531–540.
55. Birch HL, Thorpe CT, Rumian AP. Specialisation of extracellular matrix for function in tendons and ligaments. Muscles Ligaments Tendons J 2013; 3: 12–22.
56. Scheys L, Spaepen A, Suetens P, et al. Calculated moment-arm and muscle-tendon lengths during gait differ substantially using MR based versus rescaled generic lower-limb musculoskeletal models. Gait Posture 2008; 28: 640–648.
57. German AJ, Holden SL, Moxham GL, et al. A simple, reliable tool for owners to assess the body condition of their dog or cat. J Nutr 2006; 136: 2031S–2033S.